Electric Vehicle Speed Control using Self-adaptive PI Gains using PSO

Yasser Ahmed[1,2], Ayman Hoballah[1,3]

[1]Taif University –Saudi Arabia, [2]Electronic Research Institute -Egypt, [3]Tanta University-Egypt
y.abdelsalam@tu.edu.sa, ayman.hoballah@f-eng.tanta.edu.eg

Abstract: *Permanent-magnet synchronous motor (PMSM) has the capability to produce efficient performance with high torque/current and power/weight ratios. Therefore PMSM has been used in a wide range of modern variable speed AC drives such as electric vehicle (EV) applications. Because of the high nonlinearity of PMSM system modelling, the gains of PI controller have significant effects on the performance during different operating points. In this study, particle swarm optimization (PSO) technique is used to specify the optimal PI controller's gains for a wide range of operation. A comparison between fixed and variable gains is investigated. The optimal results are used to map the PI controller's gains at variable operating load speed and torque using mathematical surface fitting tool for online gains adaptation. The proposed methodology is applied on the EV as a case study at different driving cycles.*

Keywords: *Permanent-magnet synchronous motor (PMSM), Electric vehicle (EV), DTC, PI, PSO.*

1. Introduction

The EV has many advantages from the environmental and economic point of view. Therefore, many researchers are focusing on its development and performance. A well-designed robust controller should consider the system behavior improvement in steady and dynamic operating states (EV torque and speed variation requirement). The PMSM has been widely used in many applications such as EV, wind systems, and industrial robots due to its advantages of high torque-mass ratio, high power-volume ratio, and high efficiency [1]. The PMSM drives are nonlinear systems and therefore their performance can be affected by parameters values during online operation which make the control process difficult. The optimal design of simple, accurate and robust controller should be able to consider the variations in motor parameters, speed and load torque.

The gains of proportional integral (PI) controllers of PMSM derive for EV can be fixed or adaptive. The fixed gain type is simple and easy in real-time implementation but it is not suitable for high performance variable speed drive applications such as EV because its performance is sensitive to the plant parameter variations, load and speed variations. Therefore, it can be used in control application around the operating point. Adaptive gains PI controllers have to be adjusted online to enhance the performance at a wide range of operating conditions [2,3].

A self-tuning fuzzy controller used to adjust the gains for speed control of induction motor based on indirect field oriented control. A comparison between the results of fixed gain and the self-tuning fuzzy controller demonstrates smaller overshoot and faster response [4,5].

A simplified adaptive neuro-fuzzy controller for speed control of induction motor is presented which based on fuzzy logic and four layers of feed-forward back propagation neural network, weights of neural network and membership functions of fuzzy logic are tuned online for speed control using speed error as input [6,7].

An adaptive neuro-fuzzy controller (NFC) based direct torque control (DTC) applied for induction motors is proposed. The methodology based on the adjustment of the parameters of the NFC for minimizing the error between the actual acceleration and the reference value. In addition to tuning the parameters of NFC, an online hysteresis band limits adjustment for torque hysteresis controller is used to minimize the steady state torque ripples [8].

A modified harmony search algorithm and general type-2 fuzzy logic controller used for tuning PI controller gains to consider the variation in the operating condition like load and speed requirement [9]. PSO has been used as optimization technique for adaptation of PID controller gains. PSO application for online adaptation of PI speed controller with variable PMSM moment of inertia based on field oriented control is presented in [10,11,12].

Speed control of EV using PMSM and online variable PI controller gains based on DTC scheme proposed in this paper. PSO has been used to search the optimal gains of the speed, flux and torque controllers of PMSM drive at many operating conditions of speed and load variations. The optimal gains of PI controllers estimated by PSO for the speed outer loop and the two inner loops flux and torque used to estimate the control surface for each controller in a wide range of operating conditions. Then, the control surface used to generate variable PI controller's gains as a function of speed, torque and flux error to control the motion of EV reducing the speed tracking error. The proposed methodology is tested at variety of standard deriving cycles.

2. System Modeling

The system under investigation of the EV speed control

using DTC of PMSM presented in Fig. 1. The system model consists of PMSM model, DTC model, and vehicle model. The controlling system contains one outer loop for speed control (PI-1) and two inner PI controllers' loops for torque (PI-2) and flux (PI-3). The output of the inner controllers (u_{d-q}) used for generation of space vector modulation switching signals ($S_{A,B,C}$). The modulation switching signals used to control the out voltage ($V_{A,B,C}$) of the three-phase inverter. The PSO used to optimize the gains for all controllers based on variety of operating conditions of speed (w_r) and torque (T_e). The next sections describe the modeling of each part.

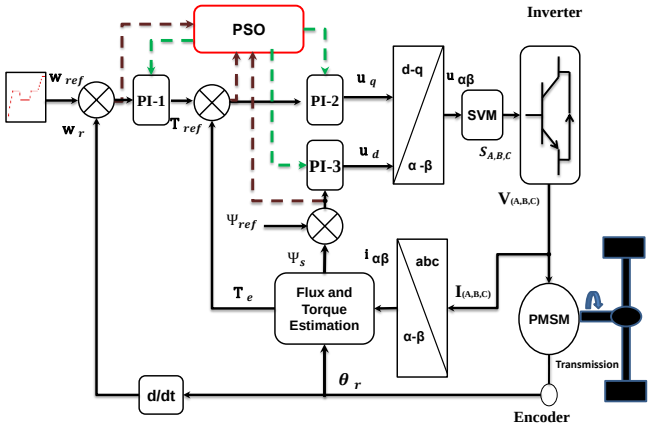

Fig. 1. The test system model

2.1. Modeling of PMSM

The mathematical model of PMSM is formulated based on a surface-mounted type. The model can be described by the following equations in a direct-quadratic synchronously rotating reference frame (*d-q*) [13].

$$u_d = R_s.i_d + \frac{d\psi_d}{dt} - w_r\psi_q \quad (1)$$

$$u_q = R_s.i_q + \frac{d\psi_q}{dt} + w_r\psi_d \quad (2)$$

$$\psi_d = L_d.i_d + \psi_{pm} \quad (3)$$

$$\psi_q = L_q.i_q \quad (4)$$

$$T_e = \frac{3}{2}P\,(\psi_d.i_q - \psi_q.i_d) \quad (5)$$

$$T_e = \frac{3}{2}\frac{1}{Ls}P|\psi_s||\psi_m|\sin\delta \quad (6)$$

$$T_e = \frac{3}{2}P\,(\psi_\beta.i_\alpha - \psi_\alpha.i_\beta) \quad (7)$$

where u_d and u_q are the d-axis and q-axis input voltage components, i_d and i_q are the d-axis and q-axis rotor current components, R_s is the stator resistance, $w_r$is the actual rotor speed, ψ_d and ψ_q are the stator flux components in rotating d-q frame, L_d and L_q are the d-axis and q-axis components of the motor inductance, ψ_{pm} is the permanent magnetic flux, T_e is the electromagnetic torque, and P is the number of pole pairs, δ the load angle, , ψ_α and ψ_β are the stator flux components in stationary frame, i_α and i_β are the stator current components in stationary frame.

The stationary frame is preferred in DTC PMSM modeling to simplify the transformation. Equation (7) represents machine electromagnetic torque in stationary α-β coordinate.

2.2Direct torque control

The basic principle of DTC is to directly control the stator flux and the electromagnetic torque by the selection of optimum voltage vector. The voltage vector is selected according to difference between the reference and actual values of electromagnetic torque and stator flux.

Fig. *2* presents the vector of stator flux linkage, Ψ_s and the rotor flux Ψ_{pm} in the *d-q* frame.

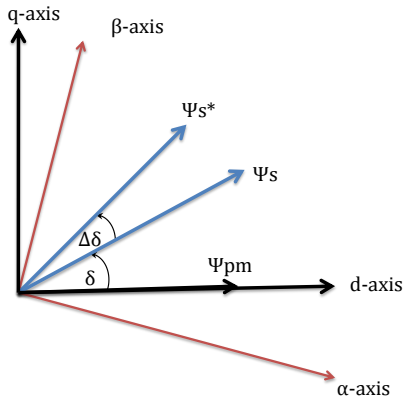

Fig. 2. The vector reference frame

The load angle between the stator flux and rotor flux (δ) is constant in the steady state operation where both stator flux and rotor flux rotate at the synchronous speed. In transient operation, δ varies due to the variation of stator and rotor flux rotating speed. The mechanical time constant of the system is very slow compared to the electrical time constant. The rotating speed of the stator flux can easily be controlled with respect to the rotor flux by selecting the voltage vector according to flux position can control the torque. The relation between the electromagnetic torque and the load angle (δ) is presented in Equation (6).

2.3Vehicle modeling

The EV modeling should consider all the forces affecting of the motion during different operating conditions. The main forces affecting the motion are the aerodynamic drag force, rolling resistance of the tires, the hill-climbing force and the gravitational force as shown in Fig. 3. The vehicle dynamic equation which describes the total force can be formulated by [14,15]:

$$F_{tract} = \frac{1}{2}\rho_{air}.A_{frontal}\,C_D V_w^2 + M_{vech}\,g\,f_r + M_{vech}g\sin\alpha + M_{vech}a \quad (8)$$

where F_{tract} is the required total force of the EV, ρ_{air} is the mass density of air, $A_{frontal}$ is the frontal area of

the vehicle, C_D is the coefficient of aerodynamic drag, V_w is the linear speed of the vehicle relative to wind, M_{vech} represents the mass of the EV, g is the acceleration of gravity, f_r represents the rolling resistance coefficient, α is the road angle, and a is the vehicle acceleration.

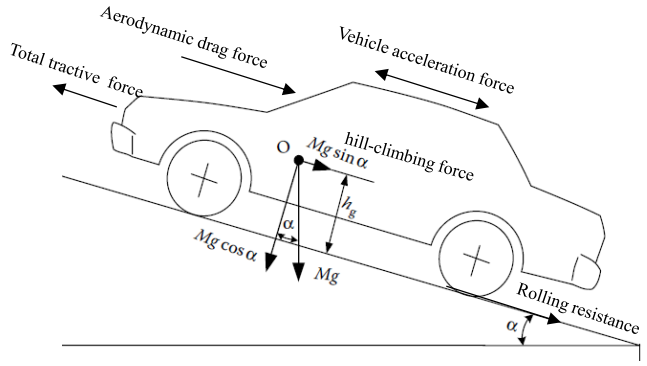

Fig. 3. Forces effecting the EV

The net force F_{tract} produces an opposite torque (T_L) against the driving motor, which can be described by equation (9). The differential equation (10) represents dynamic behavior of the combination of PMSM and EV [9,15].

$$T_L = F_{tract} \cdot \frac{r}{G} \tag{9}$$

$$\frac{dw_r}{dt} = T_e - \left(\frac{1}{J+M_{vech}\frac{r^2}{G^2}} + B\right) w_r - T_L \tag{10}$$

where r is the tire radius of the EV, G the gearing ratio and B is the motor friction coefficient.

The traction PMSM must be able to provide sufficient torque to overcome the total required force (F_{tract}) and propel the vehicle forward at a desired speed.

3. PI Controller Gain Selection using PSO

The basic idea is to adjust the gains of speed, flux, and torque controllers in order to track the reference speed at minimum error on the basis of the speed, flux and torque error as shown in Fig. 1. At each operating condition, PSO algorithm used to optimize the gains of the PI controllers for high-performance DTC drive.

3.1. Fundamentals of PSO

PSO as a famous meta-heuristic optimization algorithm is used in searching for the optimal solution within a pre-specified search space. The searching process is iteratively modify the positions of pre-specified initial solutions (particles) based on the local and global experiences of the particles in the swarm. Each particle represents the variables for the problem under investigation. The position of each particle (X_i^k) is updated in each iteration (k) based on their velocities (Y_i^k) using the following equations [16]:

$$X_i^{k+1} = X_i^k + \chi Y_i^{k+1} \tag{11}$$

$$Y_i^{k+1} = z^{k+1} Y_i^k + C_1\left(X_{li}^k - X_i^k\right) + C_2\left(X_{gi}^k - X_i^k\right) \tag{12}$$

where, X_i^k and Y_i^k are the position and velocity of particle i in iteration k. χ is a constriction factor to improve the swarm conversion. z is a weight factor for controlling the velocity of the swarm towards the optimal solution. C_1 and C_2 are generated random numbers in the range of 0 and 1.5. X_{li}^k and Y_{gi}^k are the local and global best positions of particle i at the current position in the k iteration.

3.2. Objective function and constraints

The particles in the swarm move during the optimization process in the direction of minimizing the average of the absolute speed error as an objective function (w_{er}^{av}) considering satisfaction of a group of constraints based on the problem under investigation. Constraints satisfaction is accounted using constraints violations during the optimization process specialty when all particles in the swarm are infeasible. The constraints are average error in machine flux and root main square error associated with the torque fluctuations.

Violations of constraints limits are used to penalize the objective function of the infeasible particles to move the swarm towards the feasible region. Many penalty functions are used to account the constraints violations. Penalty functions can be classified mainly into static, dynamic and adaptive Penalty functions with online parameters adaptation are most efficient and utilized ones where no user-specified parameters are specified. A penalty function with online-parameters adaptations based algorithm is introduced and used in many applications [17].

In this paper, each particle represents the gains of the speed, toque and flux controllers. The original objective is considered as minimizing of the mean absolute of speed tracking error over the time horizon. The constraints taken into account are the mean absolute of flux error and the mean absolute of torque error. The constraints violations are considered using a self-adaptive penalty formulation for the infeasible solutions in swam where no need for parameters estimation in the formulation [18]. A modified fitness function ($F_i^k = f(f_i^k, C_i^k)$is formulated base on the normalized original objective function (f_i^k) and normalized average constraints violations (C_i^k) of pre-specified error. The problem can be formulated as follows:

Minimize the average of the absolute speed error:

$$f_i^k = w_{er}^{av} \tag{13}$$

Subject to:

$$\psi_{er}^{av} = \left|\frac{\sum_{n=1}^{N}(\psi_{ref}-\psi_s)}{N}\right| < \psi_{er}^{max} \tag{14}$$

$$T_{er}^{av} = \left|\frac{\sum_{n=1}^{N}(T_{ref}-T_e)}{N}\right| < T_{er}^{max} \tag{15}$$

where ψ_{er}^{av}.and T_{er}^{av} are the average errors of stator flux and machine torque, ψ_{ref} and T_{ref} are the reference values of stator flux and torque, ψ_{er}^{max} and T_{er}^{max} are the maximum limits of the errors in stator flux and torque and N is the number of discrete values during operating time.

The iterative optimization process is shown in Fig. 4.

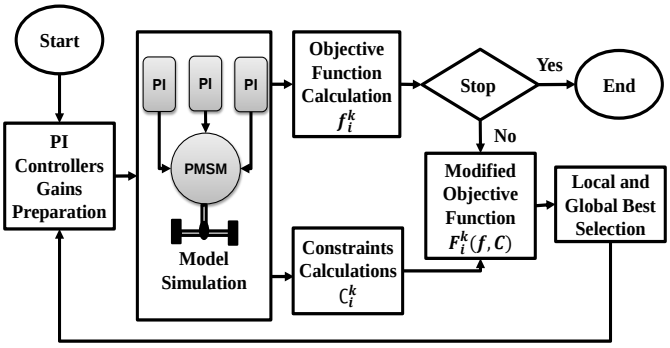

Fig. 4. Iterative optimization process using PSO

The constraints violations are used to compromise between the infeasible solutions in the swarm to push the swarm towards the feasible region based on the ratio of particles feasibility in the swarm [18]. High level of penalization based on the constraints violations is used in case of low feasible solutions ratio and with increasing of the ratio of feasible solutions in the swarm the motion of the swarm depend on the original objective function during specify the local and global best position for each particle. The target is to move in the way to minimize the original objective function without constraints violations. The selection strategy for selecting the local and global best positions, which used to modify the particle positions, presented in Fig.5.

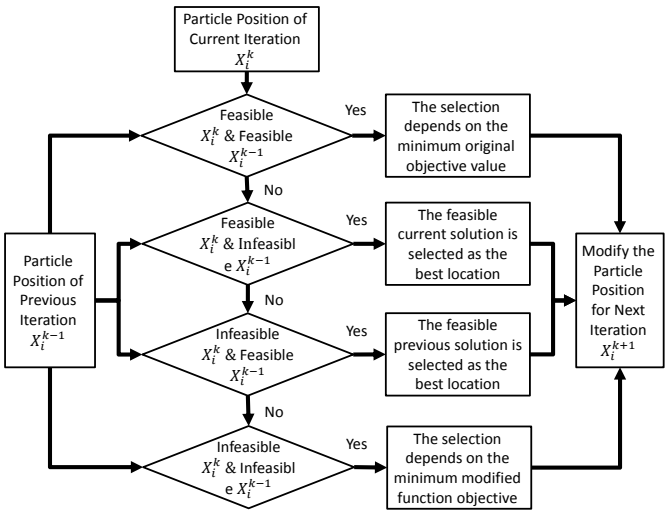

Fig.5. Selection strategy for local and best locations

In the selection strategy, the state of feasibility is used to modify the location of local and global best positions to accelerate the swarm speed towards the feasible region during the iterative process.

3.3. PSO procedure for optimal gains selection

The procedure of searching for the optimal gains using PSO can be summarized as follow:

Step 1: Specify the limits of the controller gains and formulate the objective function and constraints.

Step 2: Generate initial population for all particles within the specified limits of gains.

Step 3: Simulated the test system for each particle (solution) and calculate the objective function and constraints

Step 4: Calculate the modified objective function for each particle.

Step 5: Select or modify the local and global best particles based on the modified objective function and the feasibility of particles.

Step 6: Modify the particles positions considering variable limits.

Step 7: Check the stopping criteria and print the global best solution and if not satisfied go to step 3.

4. Simulation Results

The test system described in Fig.1 is modeled and simulated in MATLAB-SIMULINK software environment. PSO algorithm is used to optimize the speed, flux, and torque PI gains controllers. The system parameters are listed in Table I.

Table I
PMSM and EV parameters of Ford Vocus car

Motor parameters		Vehicle parameters	
R (ohm)	0.0068	Mass Mvech (kg)	1230
Ld (mH)	0.482	Frontal area Afrontal (m^2)	2.26
Lq (mH)	0.482	Tire radius r (m)	0.2
P (poles)	4	Drag coefficient (C_D)	0.324
J (kg-m^2)	0.0015	Rolling resistance coefficient (f_r)	0.01
Ym (Wb)	0.1413		

4.1 PSO application for selecting optimal PI controller gains

4.1.1 Results for Fixed and variable gains

At first case, the gains considered fixed over the simulation time for all operating points where the speed and torque considered variable. The optimal values of PI controller gains tabulated in Table (II). At second case, the gains considered variables during the simulation time. The optimal values of PI controller gains tabulated in Table (III). During simulation, there are load step changes at 0.6 sec, 1.5 sec, and 2.5 sec. There are ramp changes in the speed at 0-0.3 sec, 1-1.1 sec, 2-2.1 sec and 3-3.1 sec. Fig. 6 presents the simulation result of the optimal solution for speed and torque in the two cases.

Table II
Optimal solution with fixed PI controller gains

Speed controller		Torque controller		Flux controller	
k_p^S	k_i^S	k_p^T	k_i^T	k_p^F	k_i^F
85.63	3215.95	0.12	95.83	273.35	2975.95

Table III
Optimal solution with variable PI controller gains

Time (sec)	Speed controller		Torque controller		Flux controller	
	k_p^S	k_i^S	k_p^T	k_i^T	k_p^F	k_i^F
0 < t ≤ 0.3	189.86	5000.0	0.36	92.08	585.35	2853.08
0.3 < t ≤1	101.43	4181.97	0.68	40.12	833.84	2506.84
1 < t ≤ 1.1	200.00	3954.97	0.07	42.74	37.27	1720.56
1.1 < t ≤ 2	66.47	3492.00	0.56	79.90	1358.99	3191.17
2 < t ≤ 2.1	116.54	3242.69	0.74	60.69	796.94	2388.44
2.1 < t ≤ 3	65.94	3042.83	0.59	52.11	584.02	204.09
3 < t ≤ 3.1	173.44	3109.46	0.18	177.64	281.88	3045.05
3.1 < t ≤ 3.5	72.12	2975.80	0.44	38.06	1995.66	2386.10

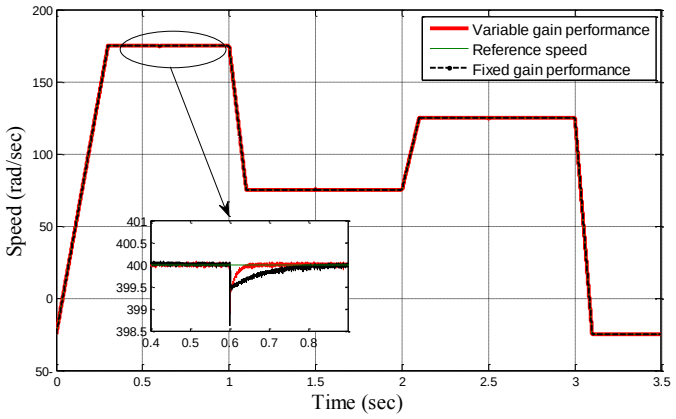

(a)

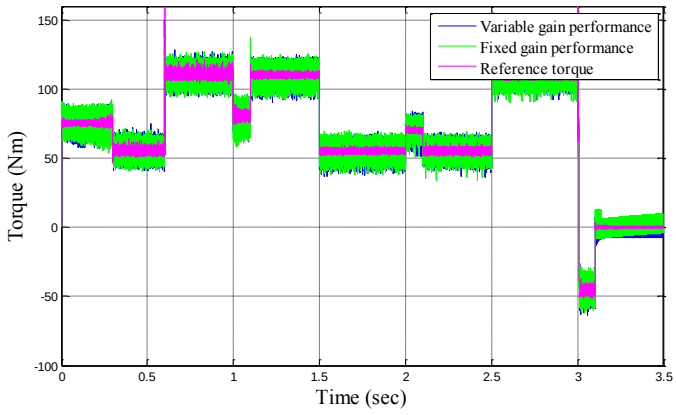

(b)

Fig. 6. Drive response with fixed and variable gains

4.1.2 Fixed and variable drive performance measurement

The performance measurement of the PMSM drive in case of fixed and variable PI controller gains based on the maximum overshoot (w_{er}^{max}) and the standard deviation (w_{er}^{sd}) of the speed tracking error. Fig. 7 refers to the in speed tracking error of both cases. From the figure, the case with PI controller variable gains drive system shows more rapid response. The drive performance quality measured and presented in Table IV. The results shows that the performance of variable PI gains drive is more accurate and track the require speed with less tracking error and less speed overshoot.

$$w_{er}^{max} = \max(w_{er}) \tag{16}$$

$$w_{er}^{sd} = \sqrt{\sum_1^n \frac{(w_{er} - w_{er}^{av})^2}{n}} \tag{17}$$

Table IV
Drive Performance Measurement

	Variable gain	Fixed gain
w_{er}^{av}	0.0364	0.0882
ψ_{er}^{av}	0.0026	0.0031
T_{er}^{av}	4.2193	5.188
w_{er}^{sd}	0.0859	0.2410
w_{er}^{max}	1.0471	2.4110

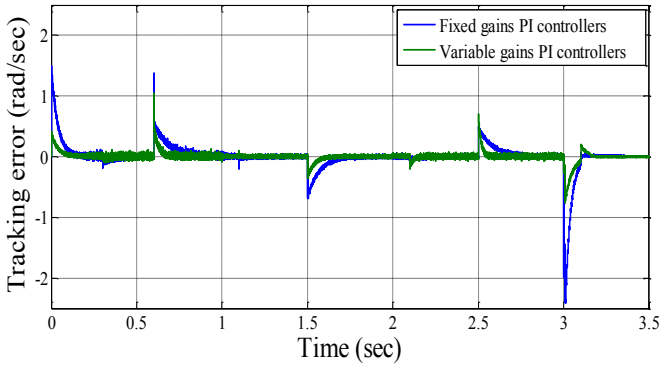

Fig. 7. Drive tracking error with fixed and variable gains

4.2 EV speed control

The results indicates that the operation with variable gains PI controllers is more efficient than the operation in case of fixed gains PI controllers.

The variable gains PI controller's data used to build surface equations, which represent the relationship between inputs and output of each PI controller to be applicable for different operating points of speed and torque. Surface fitting mathematic tool used to interpolate the optimal gain values of PI controllers. Fig. 8 maps the relation between the inputs of speed controller (PI-1) (speed error (wer) and integration of speed error (swer)) and the reference torque (Tref) as an output.

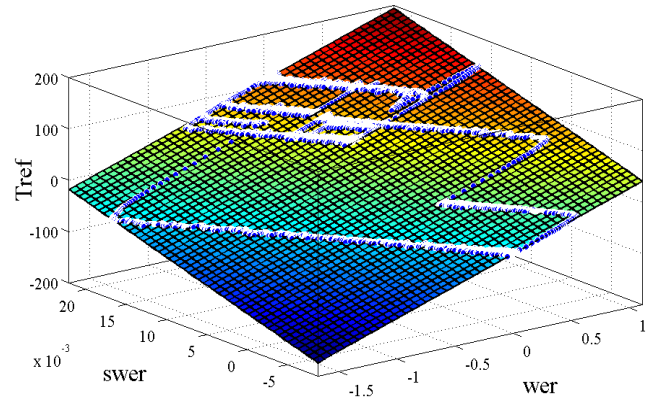

(a)

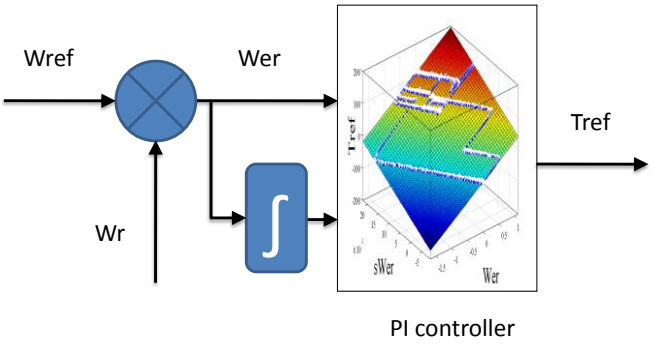

(b)

Fig. 8 Speed controller inputs-output relation

The same process is applied for torque and flux PI controllers. Then the estimated relations of speed, flux and torque controller listed in Equations (18-20) are applied for controlling the speed of EV. The accuracy of the proposed methodology of gains estimation is investigated using two different standard deriving cycles.

The surface equations represent the speed, torque and flux time varying gains PI controllers are:

$$T_{ref} = 184.1\, w_{er} + 5482 sw_{er} - 82.27\, {w_{er}}^2 - 2220\, w_{er} sw_{er} + 5.11e4\, {sw_{er}}^2 \quad (18)$$

$$V_q = 0.285\, T_{er} + 4.271\, sT_{er} + 5.33e-5\, {T_{er}}^2 + 0.299\, T_{er} sT_{er} + 217.4\, {sT_{er}}^2 \quad (19)$$

$$V_d = 5.275\, \Psi_{er} + 0.581\, s\Psi_{er} - 0.528 {\Psi_{er}}^2 - 2.32\, \Psi_{er} s\Psi_{er} - 0.1998\, {s\Psi_{er}}^2 \quad (20)$$

The obtained surface equations representing the PI controllers applied on two different test cycles. The selected driving test cycles are the urban dynamometer-driving schedule (UDDS) and the highway driving cycle test (HWDCT) which used to test the EV drive system.

4.2.1 Urban dynamometer driving schedule

Fig. 9 presents the EV system response obtained over the UDDS cycle. The motor drive has the capability to track the reference speed with speed tracking error of $-1.49 * 10^{-5}$ km/h and maximum speed tracking error of $-7.62 * 10^{-2}$ km/h. The motor torque varies within the motor rated torque with a maximum overshoot value of 84.97 N.m.

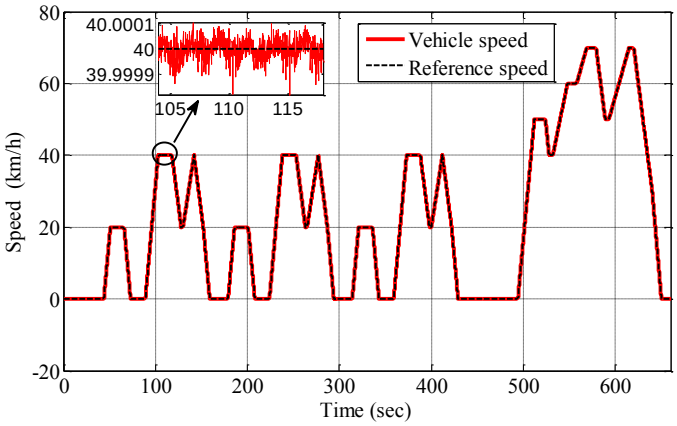

(a)

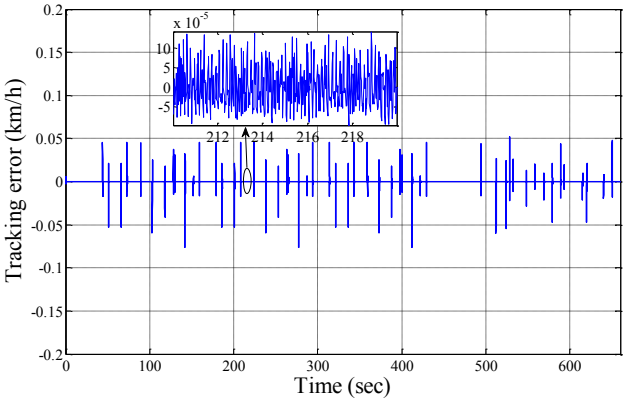

(b)

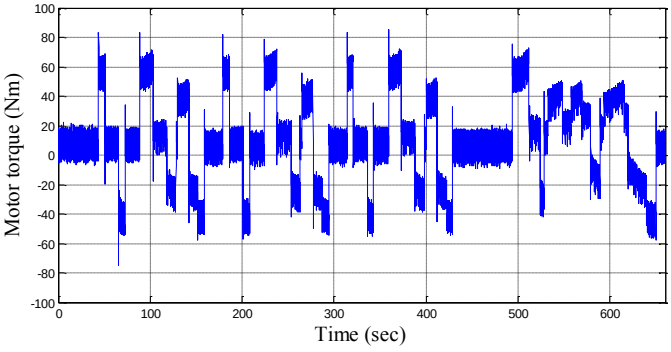

(c)

Fig. 9. Vehicle response in case of UDDS

4.2.2 Highway driving cycle test

Fig. 10 shows the vehicle response derived over a HWDCT cycle. The motor drive has the capability to track the reference speed with speed tracking error of $-5.33 * 10^{-6}$ km/h and maximum speed tracking error of

$-7.87 * 10^{-2}$ km/h. The motor torque varies within the motor rated torque with a maximum overshoot value of 90 N.m.

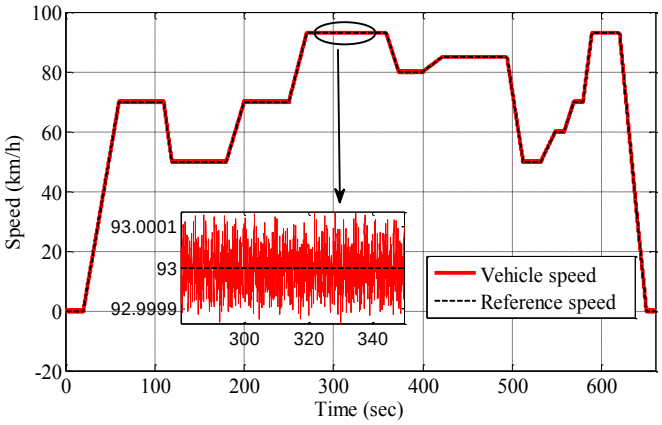

(a)

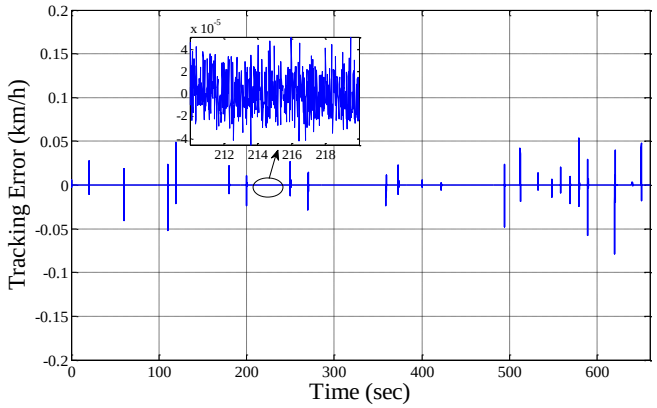

(b)

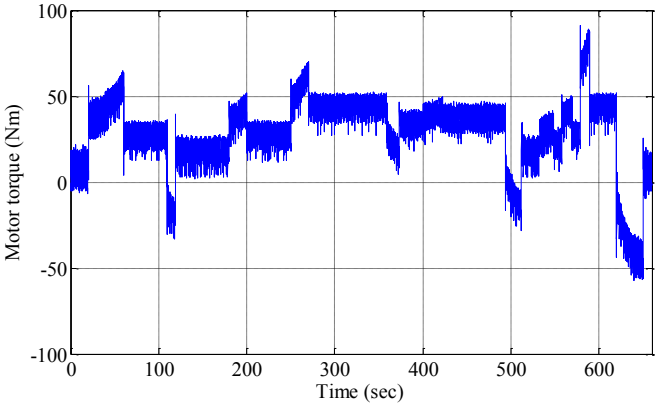

(c)

Fig. 10. Vehicle response in HWDCT

5. Conclusion

The paper presents modeling, simulation and comparison of a speed control of PMSM drive based on DTC in case of variable and fixed gains PI controllers at different operating states. The parameters of outer PI speed and the inners flux and torque controllers are optimized using PSO. The results from the comparison shows a smaller overshoot and faster response of the variable gains PI controllers over fixed ones. A mathematical model is obtained using mathematical surface fitting tool to map the PI controller's gains adaptation for variable operating load speed and torque. The obtained mathematical model is applied on the EV as a case study at two different driving cycles (UDDS and HWDCT|). The results clarify that the PMSM drive with the obtained PI mathematical model able to track the electric vehicle load requirements with a very low tracking speed error in both UDDS and HWDCT driving cycles.

References

[1] Hui Deng, Guang-Zhong Cao, Su-Dan Huang, Lai-Juan Shi and Zhi-Ming He, "*A sensorless vector strategy for the PMSM using improved sliding mode observer and fuzzy PI speed controller*," In: 6th International Conference on Power Electronics Systems and Applications (PESA), 2015, p. 1-6, Hong Kong.

[2] J. W. Jung, V. Q. Leu, T. D. Do, E. K. Kim and H. H. Choi, "*Adaptive PID Speed Control Design for Permanent Magnet Synchronous Motor Drives*," In: IEEE Transactions on Power Electronics, vol. 30, no. 2, p.. 900-908, Feb. 2015.

[3] A. Rahimi, F. Bavafa, S. Aghababaei, M.H. Khooban, S.V. *Naghavi*, " *The online parameter identification of chaotic behaviour in permanent magnet synchronous motor by self-adaptive learning bat-inspired algorithm, "* In*:* Int J Electr Power, 78 (2016), p. 285–291.

[4] M. Masiala, B. Vafakhah, J. Salmon and A. M. Knight, "*Fuzzy Self-Tuning Speed Control of an Indirect Field-Oriented Control Induction Motor Drive*," In: IEEE Transactions on Industry Applications, vol. 44, no. 6, Nov.-Dec. 2008, p. 1732-1740.

[5] C. L. Tseng, S. Y. Wang, S. C. Chien and C. Y. Chang, "*Development of a Self-Tuning TSK-Fuzzy Speed Control Strategy for Switched Reluctance Motor*," In IEEE Transactions on Power Electronics, vol. 27, no. 4, April 2012, p. 2141-2152.

[6] M. N. Uddin, Z. R. Huang and A. B. M. S. Hossain, "*Development and Implementation of a Simplified Self-Tuned Neuro–Fuzzy-Based IM Drive*," In: IEEE Transactions on Industry Applications, vol. 50, no. 1, Jan.-Feb. 2014, p. 51-59.

[7] N. Ozturk, E. Celik, "*Speed control of permanent magnet synchronous motors using fuzzy controller based on genetic algorithms*," Int. J. Electr. Power Energy Syst., 43 (1) (2012), p. 889–898.

[8] M. Hafeez, M. N. Uddin, N. A. Rahim and H. W. Ping, "*Self-Tuned NFC and Adaptive Torque Hysteresis-Based DTC Scheme for IM Drive*," In: IEEE Transactions on Industry Applications, vol. 50, no. 2, March-April 2014, p. 1410-1420.

[9] M. H. Khooban, T. Niknam and M. Sha-Sadeghi, "*Speed control of electrical vehicles: a time-varying proportional–integral controller-based type-2 fuzzy logic*," In: IET Science, Measurement & Technology, vol. 10, no. 3, May 2016, p. 185-192.

[10] X. Wang, B. Ufnalski and L. M. Grzesiak, "*Adaptive speed control in the PMSM drive for a non-stationary repetitive process using particle swarms*," In: 10th

International Conference on Compatibility, Power Electronics and Power Engineering (CPE-POWERENG), Bydgoszcz, 2016, p. 464-471.

[11] S. Cao, J. Tu and H. Liu, "*PSO algorithm-based robust design of PID controller for PMSM*," In: Sixth International Conference on Natural Computation, Yantai, Shandong, 2010, p. 3513-3517.

[12] M. Calvini, M. Carpita, A. Formentini and M. Marchesoni, "*PSO-Based Self-Commissioning of Electrical Motor Drives*," In: IEEE Transactions on Industrial Electronics, vol. 62, no. 2, Feb. 2015, p. 768-776.

[13] Y. Zhang, J. Zhu, W. Xu and Y. Guo, "*A Simple Method to Reduce Torque Ripple in Direct Torque-Controlled Permanent-Magnet Synchronous Motor by Using Vectors With Variable Amplitude and Angle*," in IEEE Transactions on Industrial Electronics, vol. 58, no. 7, pp. 2848-2859, July 2011.

[14] S. Wahsh, Y. Ahmed, E. AboElzahab, and M. AbdElAziz, "*Plug in parallel hybrid electric vehicle or hybrid electric vehicle*", In: JEE, Vol. 14, 2014, edition 3, p 324-313.

[15] Q. Huang, Z. Huang and H. Zhou, "*Nonlinear optimal and robust speed control for a light-weighted all-electric vehicle*," In: IET Control Theory & Applications, vol. 3, no. 4, April 2009, p. 437-444.

[16] J. Kennedy and R. Eberhart, "*Particle swarm optimization*," In: Neural Networks, 1995. Proceedings, IEEE International Conference on, Perth, WA, 1995, vol.4, p. 1942-1948.

[17] B. Tessema, and G. G. Yen, "*A Self Adaptive Penalty Function Based Algorithm for Constrained Optimization*," In: IEEE Congress on Evolutionary Computation, CEC 2006,16-21 July 2006,Vancouver, BC, Canada, p. 246–253.

[18] A. Hoballah and I. Erlich, "*PSO-ANN approach for transient stability constrained economic power generation*," In: PowerTech, 2009 IEEE Bucharest, Bucharest, Romania, 28 June – 2 July 2009, p. 1-6.